Calculation to Determine the Optimal Shock Absorber of a Bus Driver Seat's Suspension System

Ngoc Dai Pham[1] and Huu Nhan Tran[1,*]

ARTICLE INFO

Article history:
Received: 17 July 2023
Revised: 15 November 2023
Accepted: 16 December 2023
Online: 20 June 2024

Keywords:
Bus drive seat
Optimal shock absorber
Seat suspension
Harmonic excitation
Random excitation

ABSTRACT

The influences of natural frequency f_{nse}, damping ratio of bus driver's seat suspension system on driver's comfort is investigated by the quarter-car 2DOF model, the frequency weighted acceleration parameter according to ISO-2631 standard is used to evaluate the comfort. Based excitations in the forms of harmonic and random are determined based on the experimental acceleration a_{z_floor} using the measuring device VM31. The results show that the optimal damping ratio determined with low f_{nse} is always smaller than the case with high f_{nse} for both the cases of harmonic and random excitations. The obtained comfort with low f_{nse} is always 30.2% and 47.1% better than that of high f_{nse} for the cases of harmonic and random, respectively. The optimal damping ratios for the random excitation case are always lower than their values for the harmonic case. In the case of low f_{nse}, the comfort is improved by 7.64% and 24.19% compared with their average values in the entire damping ratio domain, corresponding to the harmonic and random excitations, respectively. However, corresponding to the high f_{nse} case, the obtained comfort is lower and improved to only 3.37% and 6.44%, respectively.

1. INTRODUCTION

Currently, issues related to vehicles in general and cars in particular are of great concern, specifically electrification, finding alternative fuels for fossil fuels, and improving drivers' health under vibration [1 - 4]. This research aims to improve the responses of bus drivers to vibration by optimizing the seat suspension system. People working on vehicles can't avoid being affected by vibrations. Vibration can come from the engine, from the rough road surface, or from the inertia of the process of changing working state, ... Normally, people operate and control vehicles in a sitting state, and the vibration in this sitting position according to [3, 4] is a form of whole-body vibration. One of the objects subjected to whole-body vibration is of primary concern is the bus driver because of the nature of the job, which must be exposed to continuous vibrations for a long time. This exposure causes many dangerous occupational diseases in bus drivers and has been statistically and investigated [5-7]. Commonly reported problems are motion sickness, headaches, and nausea, which have been reported in studies [3, 4, 8]. More serious diseases involving the cervical vertebrae, discs, and muscles of the back near the pelvis are of concern [9-11]. In addition, many studies have shown that whole-body vibration affects internal organs, physiological systems, digestive systems and reproductive organs of women [3, 4, 6].

Seat suspension systems are commonly used to reduce vibrations transmitted to the driver's body in both buses, long-distance large trucks, dump trucks, excavators working in construction sites, tunnels mines [12-14]. In order to ensure the most efficient working of the seat suspension system under each individual condition, studies to optimize the seat suspension specifications are carried out to investigate. Specifically, a study compares the effectiveness of vibration reduction in passive, semi-active, and active seats [13] and between different active forms [15]. A study on optimizing a dump truck seat suspension system through optimization of seat cushion, spring and shock absorber parameters are carried out [14, 16]. Driver vibration control using a 5DOF model, including a 4DOF split driver's body model [17, 18]. Optimize driver comfort and the seat suspension's relative displacement using a 8DOF quarter-car model [19, 20] and a 13DOF whole-car model [21].

This study determines the optimal damping ratio parameters of the bus driver's seat suspension system with two values of low and high natural frequencies. Calculations are carried out under the effect of harmonic excitation. The parameters to evaluate the comfort, the suspension dynamic deflection of the seat suspension system are analyzed as the basis for determining the optimal shock absorber corresponding to two values of the natural frequency of the seat. In addition, the comfort of the bus driver's seat with the

[1]*Faculty of Transportation Engineering, Ho Chi Minh City University of Technology (HCMUT) – Vietnam National University Ho Chi Minh City, 268 Ly Thuong Kiet Street, District 10, Ho Chi Minh City, Vietnam.*
**Corresponding author:* Huu Nhan Tran; Phone: +84-838-963-963; Email: thnhan@hcmut.edu.vn.

suspension system with the obtained optimal damping ratio is also analyzed based on the obtained results in the case of random excitation. In which, the random displacement signal is determined by a random mathematical model based on the random acceleration of the floor obtained by experiment.

2. EXPERIMENTAL METHODS

Wenda Gi.34 bus, gross weight 12.5 (ton), length 12.2 (m), 6-cylinder diesel engine, Figure 1, used as the object of vibration measurement investigation. In particular, the vibration of the floor at the driver's sitting position is the measured factor in the study. Measurements are taken on a daily working route with the experimental apparatus setting up shown in Figure 2. The data collection is carried out on a 40 (km) long route with an average speed 40 (km/h).

Fig. 1. The bus Wenda Gi.34.

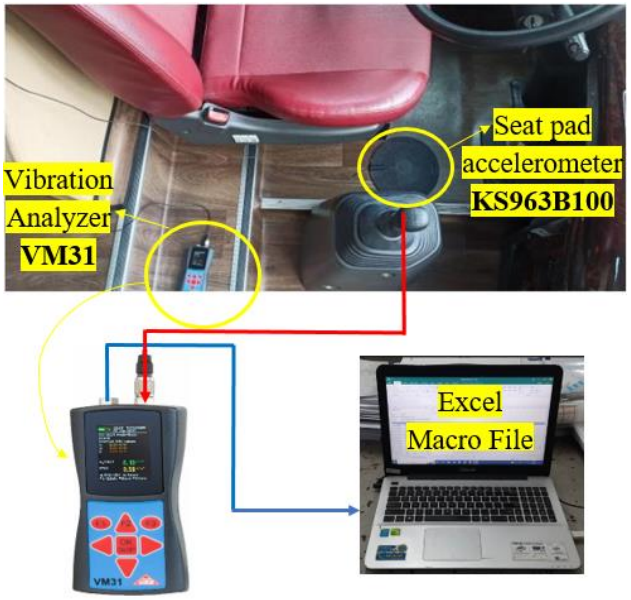

Fig. 2. Experimental apparatus setup.

When performing floor vibration acceleration measurement, the measuring device VM31 uses the measurement mode "General vibration acceleration measurement" to receive acceleration data a_{z_floor} from sensor KS963B100 in the frequency range from 0.2÷1500 (Hz) and stored as interval root mean square (IRMS), Figure 2. The KS963B100 sensor has specifications as: Measuring range ±60g, Voltage sensitivity 100mV/g, Linear frequency range 0.5÷1000 (Hz).

The KS963B100 sensor collects floor acceleration data, which is then used to determine the displacement excitation of the floor.

3. SIMULATION MODEL AND PARAMETERS

3.1. Simulation model

3.1.1. Driver seat dynamic 2DOF model

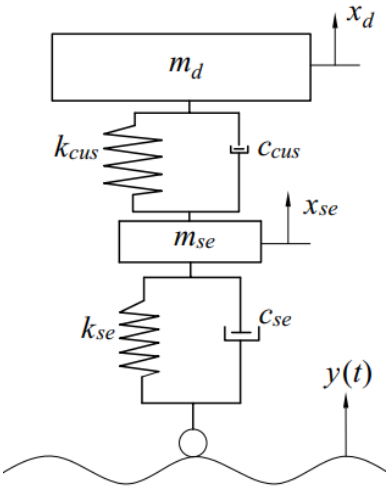

Fig. 3. Driver seat dynamic 2DOF model.

where:

m_{se}, m_d: mass elements of the seat and the driver, respectively (kg)

c_{se}, c_{cus}: damping coefficients of the seat suspension system and the cushion, respectively (Ns/m)

k_{se}, k_{cus}: spring stiffnesses of the seat suspension system and the cushion, respectively (N/m)

x_{se}, x_d: vertical displacements of the seat and the driver, respectively (m)

$\dot{x}_{se}, \dot{x}_d$: vertical velocities of the seat and the driver, respectively (m/s)

$\ddot{x}_{se}, \ddot{x}_d$: vertical accelerations of the seat and the driver, respectively (m/s2)

$y(t)$: based excitation (m)

g: gravity acceleration (m/s^2)

The model of the 2DOF driver's seat suspension system is shown in Figure 3. In which, the seat mass element m_{se} is linked to the floor of the vehicle through the k_{se} - c_{se} seat suspension system. The driver mass element m_d is linked to the seat frame through the k_{cus} - c_{cus} seat cushion.

3.1.2. Mathematical model

The quarter-car 2DOF dynamic model is employed to determine the optimal damping coefficients corresponding to the low and high natural frequencies of the seat suspension system. This is a simple model and can

completely help determine the vibration evaluation indexes of the driver seat for both random and harmonic excitation cases.

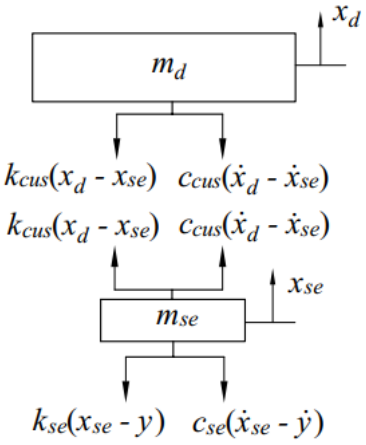

Fig. 4. Free body diagram of the mass elements.

Applying the Newton's second law according to the free body diagram in the mass elements m_{se}, m_d in Figure 4, we obtain the differential equations (1):

$$[m]\left[\ddot{X}\right]+[c]\left[\dot{X}\right]+[k][X]=[F] \qquad (1)$$

where:

$[m],[c],[k]$: matrices of mass, damping coefficient, and spring stiffness, respectively;

$[X],\left[\dot{X}\right],\left[\ddot{X}\right]$: vectors of displacement, velocity and acceleration, respectively;

$[F]$: vector of applied force

$$[m]=\begin{bmatrix} m_d & 0 \\ 0 & m_{se} \end{bmatrix}$$

$$[c]=\begin{bmatrix} c_{cus} & -c_{cus} \\ -c_{cus} & c_{cus}+c_{se} \end{bmatrix}$$

$$[k]=\begin{bmatrix} k_{cus} & -k_{cus} \\ -k_{cus} & k_{cus}+k_{se} \end{bmatrix}$$

$$[F]=\begin{bmatrix} 0 \\ c_{se}\dot{y}+k_{se}y \end{bmatrix}$$

$$\left[\ddot{X}\right]=\begin{bmatrix} \ddot{x}_d \\ \ddot{x}_{se} \end{bmatrix},\left[\dot{X}\right]=\begin{bmatrix} \dot{x}_d \\ \dot{x}_{se} \end{bmatrix},[X]=\begin{bmatrix} x_d \\ x_{se} \end{bmatrix}$$

3.2. Calculation parameters

3.2.1. Input parameters

Input parameters of the model, Figure 3, are summarized in Table 1. In which, the spring stiffness k_{se}, the damping coefficient c_{se} of the seat suspension system are calculated respectively according to the natural frequency f_{nse} and damping ratio ξ_{se} [22].

Table 1. Input parameters

Symbol	Value	Unit
m_d	65	kg
m_{se}	20	kg
f_{nse}	2.5; 4.0 [22]	Hz
ξ_{se}	0.1÷0.8 [22]	-
c_{cus}	217 [14]	Ns/m
k_{cus}	58400 [14]	N/m

3.2.2. Based excitation

3.2.2.1. Random excitation

The pavement random function according to ISO 8608 is employed to describe the random displacement signal profile of the bus floor $y_r(t)$ (2) [23].

$$y_r(t)=\sum_{1}^{N} A_i \sin\left(\Omega_i.v.t-\psi_i\right) \qquad (2)$$

where:

A_i: the i^{th} sine wave amplitude (m);

N = 500: the number of sine waves is chosen;

i = 1÷N: the i^{th} sine wave;

Ω_i : the wavenumbers Ω_i are chosen to lie at N equal intervals $\Delta\Omega$ (rad/m);

v = 40 (km/h): velocity;

t: time (s);

ψ_i: is the different sets of uniformly distributed phase angles in the range between 0 and 2π (rad).

The i^{th} sine wave amplitude A_i is determined (3) [23].

$$A_i=\sqrt{2\Phi\left(\Omega_i\right)\Delta\Omega} \qquad (3)$$

where:

$$\Phi\left(\Omega_i\right)=\Phi_0\left(\frac{\Omega_i}{\Omega_0}\right)^{-w} \qquad (4)$$

with:

Φ_0 : the value of the psd at the reference wavenumber $\Omega_0=1$ (rad/m) ;

w = 2: the drop in magnitude.

In order to determine the random excitation as the displacement variation of the floor surface over time, $y_r(t)$, from the experimental data obtained as RMS random acceleration of the floor over time, we select the excitation frequency domain in the normal range of the vehicle, from

[0.5÷20] (Hz) [13]. Using a mathematical model of the random of the pavement according to ISO 8608 [23], vary the value of the power spectral density parameter Φ_0, until we obtain the RMS value of the nearest random pavement acceleration, which is incorrect not more than 2% deviation from the average value of the experimental interval RMS acceleration. The random displacement variation over time is chosen to be used as a random excitation at the vehicle floor. Performing calculations according to Figure 5, we can determine the value of power spectral density $\Phi_0 = 5.8\text{x}10^{-8}$ (m^3/rad). The random acceleration satisfying the condition that RMS is approximately equal to the mean RMS of a_{z_floor} obtained by experiment, with an error of less than 2% according to the calculation procedure, Figure 5.

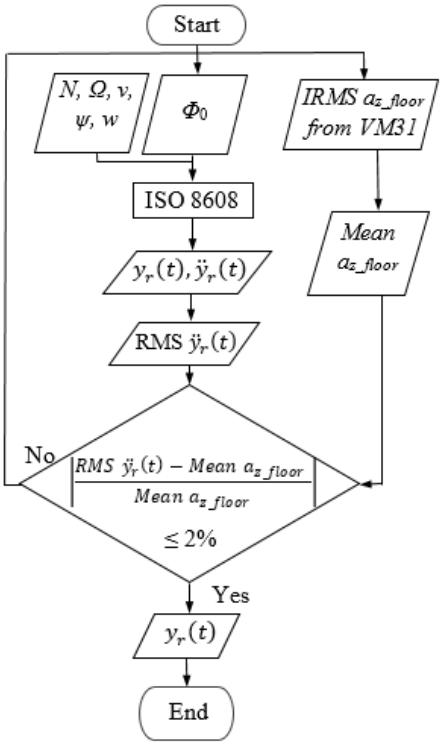

Fig. 5. Determination flowchart of random excitation.

3.2.2.2. Harmonic excitation

The input excitation $y_h(t)$ in the form of a harmonic function in the normal working frequency domain of the vehicle f [0.5÷20] (Hz) [13], Figure 6, is employed.

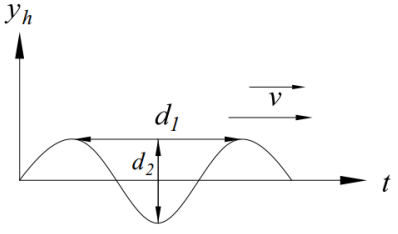

Fig. 6. Harmonic excitation [24].

The harmonic excitation in Figure 6 is described as a mathematical equation as (5) [24].

$$y_h = \frac{d_2}{2}\sin\left(\frac{2\pi v}{d_1}t\right) \quad (5)$$

where:

d_1 = 1.0 (m) : length of bump;

$d_2/2 = RMS\ y_r(t)$ (m): height of bump;

v = 0.5÷20 (m/s): velocity;

t: time (s).

The bump length is chosen as d_1 = 1.0 (m), so that the traveling velocity of the vehicle v [0.5÷20] (m/s) will correspond to the excitation frequency f [0.5÷20] (Hz) [13] according to (5).

3.3. Gain responses

At each frequency value of the harmonic excitation, the gain response of driver acceleration G_{da} and the gain response of seat suspension relative displacement G_{dz} are determined according to (6) and (7), respectively.

$$G_{da} = \frac{\max\left(\ddot{x}_d\right)}{\max\left(\ddot{y}_h\right)} w_k \quad (6)$$

where:

$\max\left(\ddot{y}_h\right)$: acceleration amplitude of the excitation (m/s^2);

w_k: frequency weighting factor.

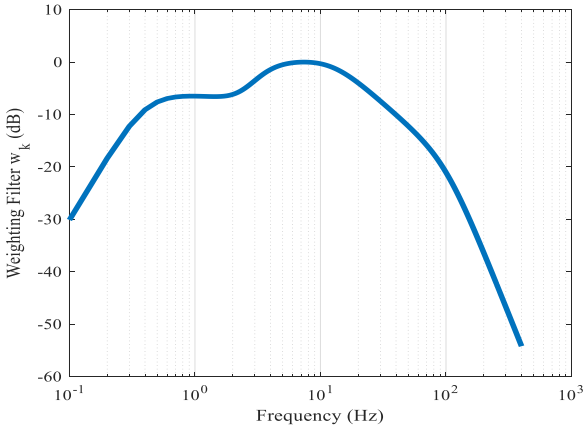

Fig. 7. Frequency weighting factor w_k [3].

$$G_{dz} = \frac{\max\left|x_{se} - y_h\right|}{\max\left(y_h\right)} \quad (7)$$

where:

x_{se}: driver's seat displacement at the steady state (m);

y_h: displacement of the harmonic excitation (m);

max(y_h): displacement magnitude of the harmonic excitation (m).

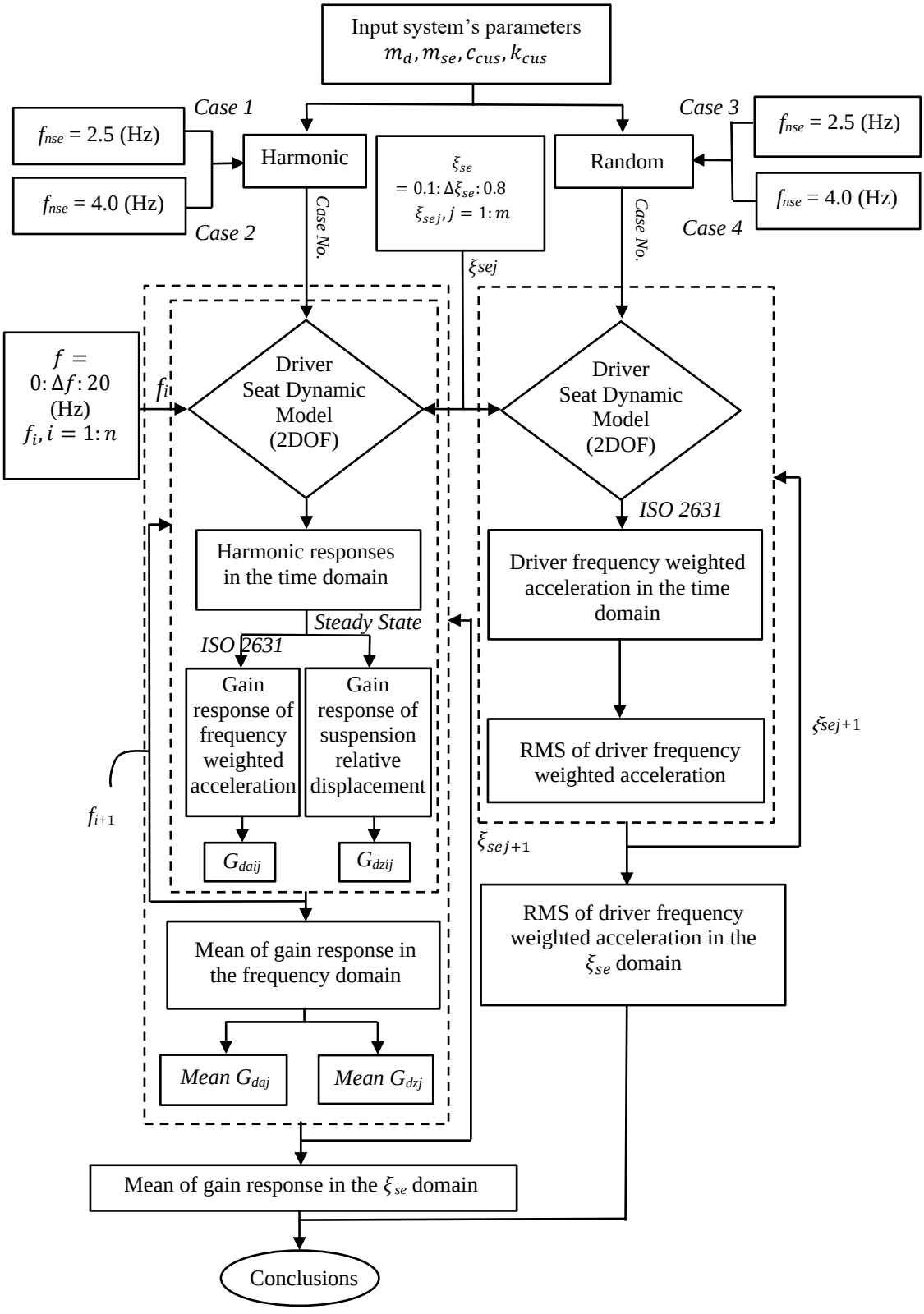

Fig. 8. Optimization calculation flowchart.

3.4. Optimization flowchart

The optimization calculation flowchart describing the general investigating process of the gain response of the driver acceleration G_{da} and the relative displacement of the seat suspension G_{dz} on the excitation frequency domain f [0.5÷20] (Hz) [13], for the cases of the seat suspension's spring and shock absorber, f_{nse} and ξ_{se}, Figure 8.

The calculation is carried out under the harmonic excitation with 2 cases of the low and high natural frequencies of the seat suspension system, f_{nse} = 2.5 (Hz) and f_{nse} = 4.0 (Hz), respectively. In which, the damping ratio of the seat suspension system ξ_{se} is in the range [0.1÷0.8] [22]. The average parameters of the driver acceleration gain response and the suspension relative displacement gain response in the frequency domain, Mean G_{da} and Mean G_{dz} are determined for each calculation case of f_{nse} and ξ_{se} values, respectively.

4. RESULTS AND DISCUSSIONS

4.1. Random excitation determination

Typical experimental RMS floor acceleration in the time domain is shown as in Figure 9, with measurement duration of about 3600 (s) over a long distance of 40 (km), the average vehicle speed 40 (km/h), average value of RMS a_{z_floor}=0.632 (m/s^2).

The measurement process is repeated 3 times, Figure 10, in which, the error between 3 measurements ranges from 0.33% (0.617 (m/s^2) at the 3rd time) to 2.76% (0.632 (m/s^2) at the 1st time) compared to the minimum value of 0.615 (m/s^2) at 2nd time. The very small error (less than 5%) between measurements shows a high similarity in the operating state daily driving of the bus when traveling on the same route, same time frame and same working load. Accordingly, the mean value of RMS a_{z_floor} over time, Mean a_{z_floor} obtained from VM31 over measurements of approximately 0.621 (m/s^2) has high reliability. It is used to determine random input displacement, Figure 5.

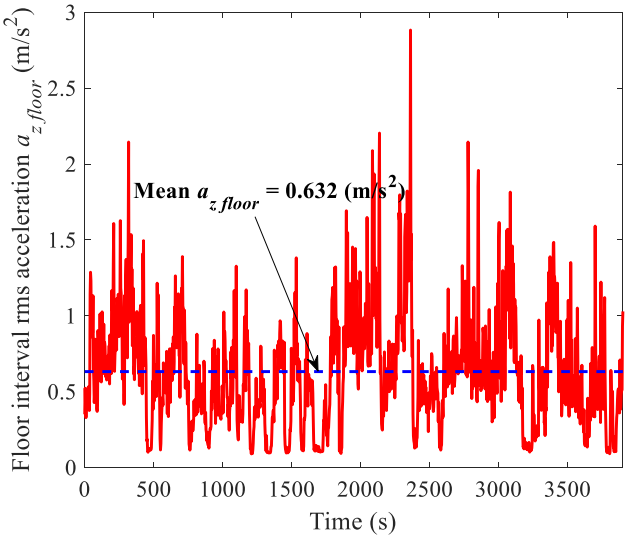

Fig. 9. Typical experimental RMS floor acceleration in the time domain.

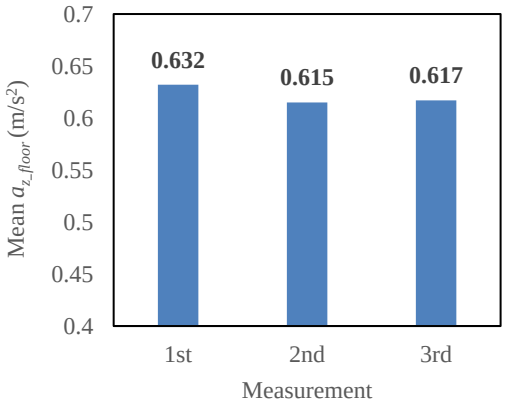

Fig. 10. Mean a_{z_floor} obtained from VM31 over 3 times of measurement.

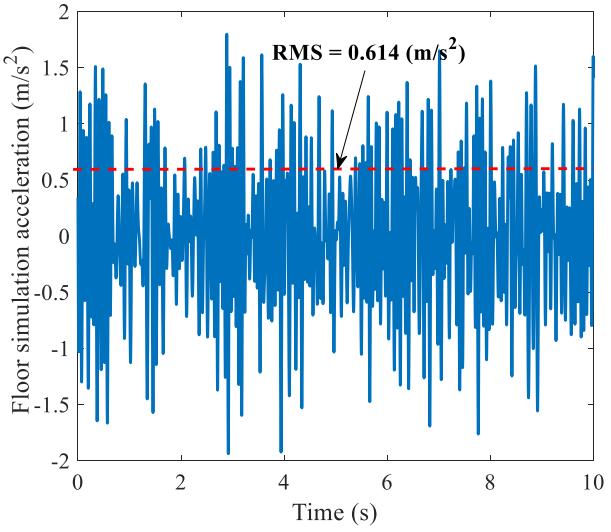

Fig. 11. The calculated acceleration of the floor in the time domain, $\ddot{y}_r(t)$.

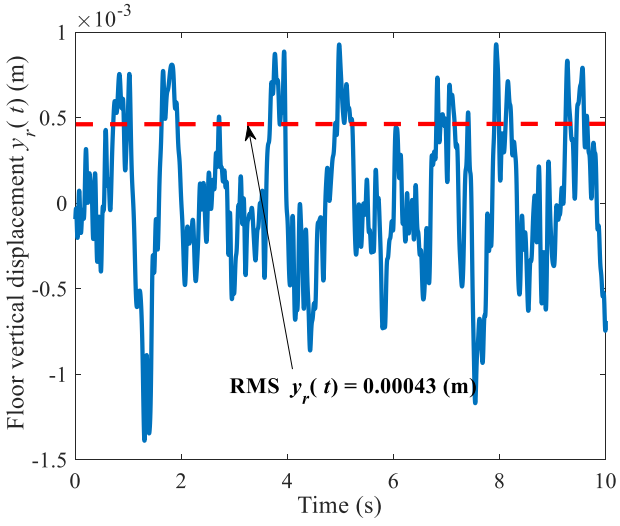

Fig. 12. The calculated random displacement of the floor in the time domain, $y_r(t)$.

Figure 11 shows that the calculated random acceleration of the floor over time is based on the average value of RMS experimental acceleration, the Mean a_{z_floor} according to the procedure shown in Figure 5. In which, the calculated random acceleration RMS value of 0.614 (m/s2) has an error of 1.13% compared with Mean a_{z_floor} = 0.621 (m/s^2). From there, the calculated random displacement of the floor over time $y_r(t)$ is determined and shown in Figure 12. The random displacement of the floor $y_r(t)$ obtained according to the procedure in Figure 5 with RMS $y_r(t) = 0.43.10^{-3}$ (m) is used as the harmonic excitation amplitude value $d_2/2$, Figure 6.

4.2. Gain responses in the frequency domain

The responses of the driver's acceleration G_{da} and the relative displacement of the seat suspension system G_{dz} in the frequency domain f [0.5÷20] (Hz) [13] are shown in Figure 13 and Figure 14. The damping ratio cases include ξ_{se}=0.1, ξ_{se}=0.4 corresponds to the seat suspension system's natural frequency of f_{nse}=2.5 (Hz) (low), and f_{nse}=4 (Hz) (high).

Figures 13 and 14 show that, in the frequency range [0.5÷5] (Hz), when considering the same natural frequency value f_{nse}, the response values G_{da} and G_{dz} reach their maximum at the resonance frequency. The smaller the damping ratio ξ_{se}, the larger the response amplitude. Specifically:

+ Figure 13: With ξ_{se}=0.1, the maximum acceleration response value G_{da_max1} is approximately 3.25 times and 2.5 times the maximum acceleration response value G_{da_max2} with ξ_{se}=0.4, respectively, according to f_{nse}=2.5 (Hz) and f_{nse}=4 (Hz).

+ Figure 14: With ξ_{se}=0.1, the maximum relative displacement response value of the seat suspension system G_{dz_max1} is approximately 3.4 times and 2.9 times, respectively, the maximum relative displacement response value of the seat suspension system G_{dz_max2} with ξ_{se}=0.4, corresponding to f_{nse}=2.5 (Hz) and f_{nse}=4 (Hz).

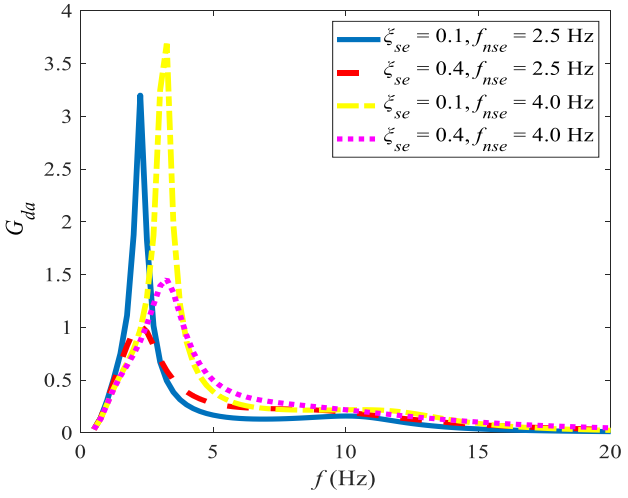

Fig. 13. Driver acceleration gain response G_{da} in the frequency domain.

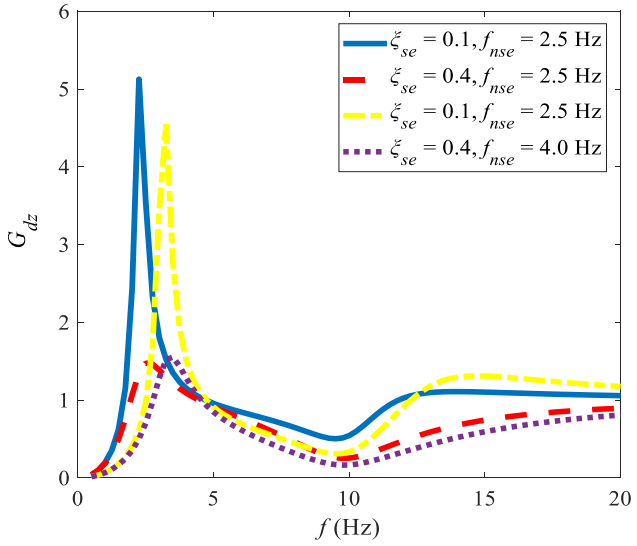

Fig. 14. Seat suspension relative displacement gain response G_{dz} in the frequency domain.

4.3. Optimal damping ratio subjected to harmonic excitation

The calculation to determine the optimal damping ratio is carried out under the harmonic excitation for each case of the natural frequency of the seat suspension system, according to the procedure shown in Figure 8. The average value of the gain response of driver acceleration, G_{da} and the gain response of seat suspension relative displacement, G_{dz} in the seat suspension damping ratio domain are determined, for each case the seat suspension natural frequencies, f_{nse}=2.5 (Hz) and f_{nse}=4.0 (Hz), are shown in Figure 15 and Figure 16, respectively.

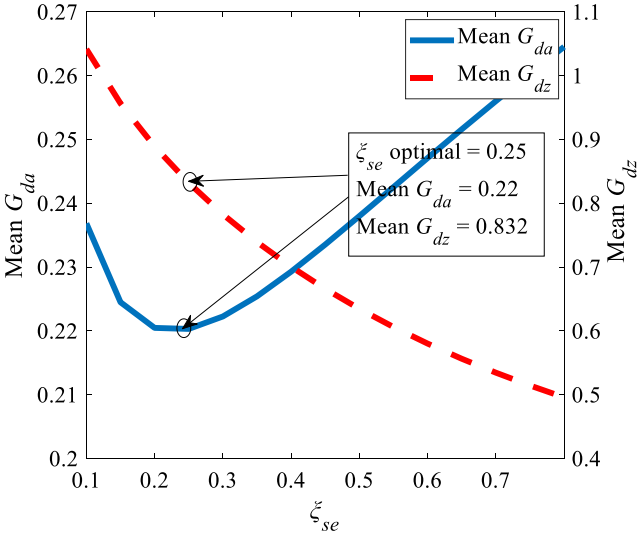

Fig. 15. The average values of the gain responses of G_{da} and G_{dz} in the ξ_{se} domain, with f_{nse}=2.5 (Hz).

The obtained results, Figure 15 shows that, when gradually increasing the value of ξ_{se} in the region [0.1÷0.25],

the Mean G_{da} value gradually decreases and reaches a minimum at ξ_{se}=0.25 with Mean G_{da}=0.22. In contrast, in the region ξ_{se} [0.25÷0.8], the Mean G_{da} value increases with ξ_{se}. The average acceleration gain response in the frequency domain reaches the minimum value at ξ_{se}=0.25 which is the value of the optimal damping ratio $\xi_{se\_opt1\_h}$. The minimum of G_{da} obtained at $\xi_{se\_opt1\_h}$ is lower than that of 7.64% in comparison with the average value, in the whole range of observed damping ratio ξ_{se}.

The average gain response of relative displacement in the frequency domain of the seat suspension system, Mean G_{dz} value always decreases with increasing damping ratio ξ_{se}, at $\xi_{se\_opt1\_h}$=0.25, Mean G_{dz} = 0.832, the harder suspension system the lower the displacement. This value is 18.52% higher than the average of Mean G_{dz} in the entire range of observed damping ratio ξ_{se}.

Similarly, the obtained results in Figure 16 show that, with f_{nse} = 4.0 (Hz), Mean G_{da} gradually decreases and reaches a minimum at ξ_{se}=0.4 with Mean G_{da}=0.315. Therefore, for f_{nse}=4.0 (Hz), the optimal G_{da} acceleration gain response is obtained at the value $\xi_{se\_opt2\_h}$=0.4. This minimum Mean G_{da} value is 3.37% lower than its average value in the entire observed damping ratio domain. In addition, it can be easily seen that in the case of lower natural frequency, the obtained comfort is 30.2% better than the case of higher natural frequency. The stiffer the suspension, the higher the acceleration obtained. In addition, the larger the damping ratio ξ_{se}, the lower the relative displacement gain response of the seat suspension, at $\xi_{se\_opt2\_h}$=0.4, Mean G_{dz} = 0.563 is 2.76% lower than the average value in the entire observed damping ratio domain. For the case of low natural frequency, f_{nse}=2.5 (Hz) at $\xi_{se\_opt1\_h}$=0.25, the obtained Mean G_{dz} is approximately 47.8% greater than f_{nse}=4.0 (Hz) at $\xi_{se\_opt2\_h}$=0.4, corresponding to the stiffer the suspension the smaller the displacement.

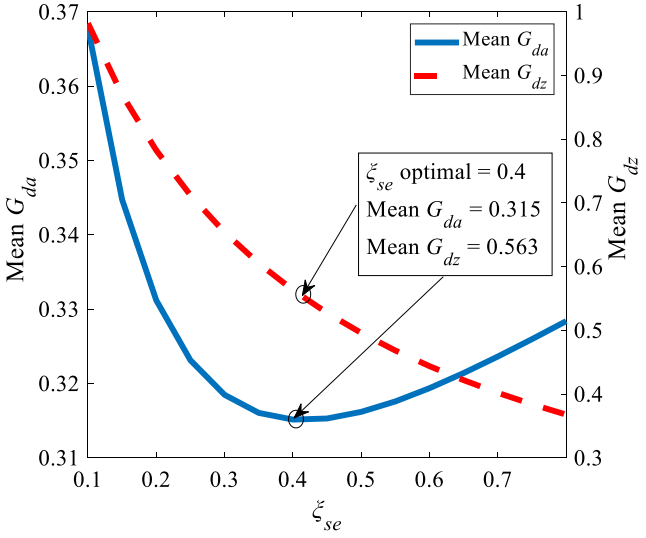

Fig. 16. The average values of the gain responses of G_{da} and G_{dz} in the ξ_{se} domain, with f_{nse}=4.0 (Hz).

4.4. Optimal damping ratio subjected to random excitation

Calculations are carried out under the random excitation to determine the driver acceleration parameters taking into account the influence of frequency weighting according to ISO-2631 [3] with two optimal cases found in section 4.2 above, Figure 17. The results show that, in the case of low natural frequency f_{nse}=2.5 (Hz), the comfort is higher than in the case of high natural one f_{nse}= 4.0 (Hz). Specifically, in the case of lower natural frequency, the obtained comfort is 47.1% better than the case of higher natural frequency, and this value is close to the case with the harmonic excitation of 30.2%.

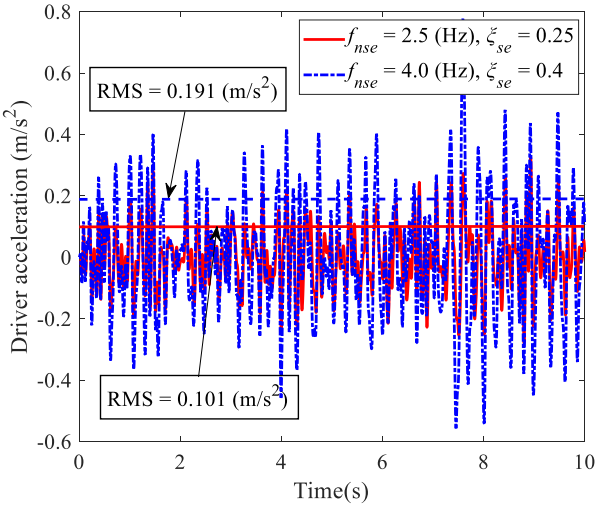

Fig. 17. Driver frequency weighted acceleration in the time domain.

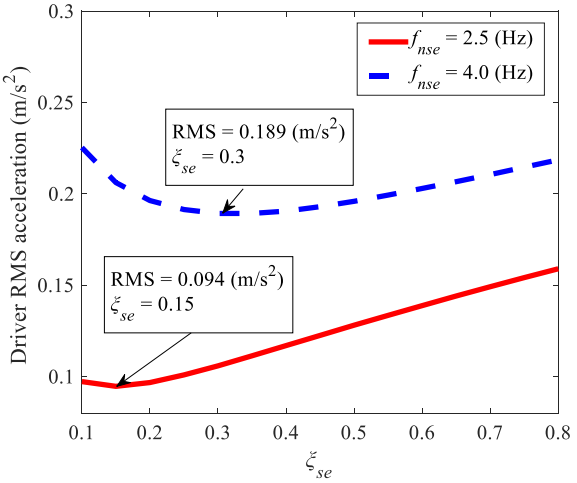

Fig. 18. RMS of driver frequency weighted acceleration in the ξ_{se} domain.

The calculation is carried out similarly under the random excitation with 2 cases of natural frequency of the suspension system, the RMS value of the driver's frequency weighted acceleration is determined, corresponding to each value of the damping ratio ξ_{se} in the observed domain. The

obtained RMS value of the driver frequency weighted acceleration in the damping ratio domain, with two cases of high and low natural frequency, is shown in Figure 18.

The obtained results show that, under the random excitation in the condition that the vehicle is moving with an average speed of 40 (km/h), the random excitation frequency is from [0.25÷20] (Hz) [13], with f_{nse}=4.0 (Hz), the RMS value of driver frequency weighted acceleration is always greater than the case f_{nse}=2.5 (Hz) for every ξ_{se} in the observed range [0.1÷0.8]. Besides, with f_{nse}=2.5 (Hz) and f_{nse}=4.0 (Hz), the RMS value of the driver frequency weighted acceleration reaches the minimum at $\xi_{se\_opt1\_r}$=0.15 and $\xi_{se\_opt2\_r}$=0.3, respectively, which is slightly smaller than the corresponding one obtained in the case of harmonic excitation. The minimum RMS values of the driver frequency weighted acceleration corresponding to the two cases of low and high natural frequencies are smaller than their average values of 24.19% and 6.44%, respectively in the entire observed damping ratio ξ_{se}.

5. CONCLUSIONS

The influences of the spring-shock absorber parameters of the seat suspension on the gain responses of the driver acceleration and relative displacement was investigated by the quarter-car 2DOF dynamic model. The calculations are carried out with 2 cases of natural frequency of the seat suspension under the harmonic and random excitations. Specifically, the random excitation is determined based on the experimental acceleration data measured at the driver's seat position according to ISO 8608. With the power spectral density Φ_0 = 5.8x10^{-8} (m^3/rad), the calculated acceleration has an error of 1.13% compared to the experimental one. The harmonic excitation with amplitude was chosen to be the RMS of the random displacement defined above.

For the case of harmonic excitation, the optimal damping ratio is determined based on the minimum average gain response of frequency weighted acceleration in the entire observed damping ratio domain. For the case of random excitation, the optimal damping ratio is determined based on the minimum RMS value of the frequency weighted acceleration in the damping ratio domain. The smaller optimal damping ratio is determined for the correspondingly lower natural frequency case. And correspondingly, for higher natural frequency, a larger optimal damping ratio is determined. In addition, with random excitation, the determined optimal damping ratio is always smaller in both low and high natural frequency cases than their optimal values determined under the harmonic excitation. The obtained results are as follows:

- Harmonic excitation: with soft seat suspension, corresponding to low natural frequency f_{nse}=2.5 (Hz) the optimal damping ratio value $\xi_{se\_opt1\_h}$=0.25 is obtained. With a harder seat suspension, corresponding to f_{nse}=4.0 (Hz), $\xi_{se\_opt2\_h}$=0.4 is obtained. In which, with f_{nse}=2.5 (Hz), Mean G_{da} value decreases to 30.2%, Mean G_{dz} value increases to 47.8% compared to when f_{nse} = 4.0 (Hz). In addition, the minimum Mean G_{da} values obtained are lower than their average values in the entire damping ratio by 7.64% and 3.37% respectively for low and high suspension natural frequencies.
- Random excitation: the soft seat suspension corresponds to the case of low natural frequency f_{nse}=2.5 (Hz), $\xi_{se\_opt1\_r}$=0.15 has a 47.1% better comfort than the harder suspension corresponding to the case f_{nse}=4.0 (Hz), $\xi_{se\_opt2\_r}$=0.3. Therefore, the optimal damping ratio determined with the random excitation is smaller than their obtained values with the harmonic excitation. Moreover, the minimum RMS values of the obtained frequency weighted accelerations are lower than their average values over the entire damping rate domain of 24.19% and 6.44%, respectively, for low and high natural frequencies of the seat suspension.

ACKNOWLEDGEMENTS

We acknowledge Ho Chi Minh City University of Technology (HCMUT), VNU-HCM for supporting this study.

REFERENCES

[1] A. Paudel and B. Marungrsi, “Analysis of the Effect of the Royal Thai Government’s Electric Vehicle Promotion Strategy on Future Energy demand, Energy Mix and Emissions from Passenger Land Transport,” GMSARN International Journal, vol. 17, pp. 184-191, 2023.

[2] D. R. Pangavhane, S. S. Harak, and P. B. Nehe, “Performance and Emission Characteristics of Straight Vegetable Oil (Svo) as Alternate Transport Fuel for Sustainable Development,” GMSARN International Journal, vol. 1, pp. 49-54, 2007.

[3] International Organization for Standardization (ISO), 1997. “Mechanical Vibration and Shock - Evaluation of Human Exposure to Whole-body Vibration. Part 1: General Requirements.” Standard No. ISO 2631-1: 1997. ISO, Geneva, Switzerland.

[4] M. J. Griffin, Handbook of Human Vibration, Academic Press Inc, London, 1990.

[5] H. Seidel and R. Heide, “Long-term effects of whole-body vibration: a critical survey of the literature,” International Archives of Occupational and Environmental Health, vol. 58, pp. 1-26, 1986.

[6] H. Seidel, “Selected Health Risks Caused by Long-Term, Whole – Body Vibration,” American Journal of Industrial Medicine, vol. 23, pp. 589-604, 1993.

[7] B. Wikström, A. Kjellberg, and U. Landström, “Health effects of long-term occupational exposure to whole-body vibration: A review,” International Journal of Industrial Ergonomics, vol. 14, pp. 273-292, 1994.

[8] M. H. U. Bhuiyan, M. Fard, and S. R. Robinson, “Effects of whole-body vibration on driver drowsiness: A review,” Journal of Safety Research, vol. 81, pp. 175-189, 2022, doi: 10.1016/j.jsr.2022.02.009.

[9] D. J. Park, J. W. Lee, J. H. Park, J. T. Song, S. J. Ahn, and W. B. Jeong, “Neck/shoulder muscle fatigue of military vehicle drivers exposed to whole-body vibration on field terrain

road," International Journal of Automotive Technology, vol. 21, no. 1, pp. 115–121, 2020, doi: 10.1007/s12239-020-0012-0.

[10] S. Amiri, S. Naserkhaki, and M. Parnianpour, "Effect of whole-body vibration and sitting configurations on lumbar spinal loads of vehicle occupants," Computers in Biology and Medicine, vol. 107, pp. 292-301, 2019, doi: 10.1016/ j.compbiomed. 2019. 02. 019.

[11] F. Y. Lan, Y. W. Liou, K. Y. Huang, H. R. Guo, and J. D. Wang, "An investigation of a cluster of cervical herniated discs among container truck drivers with occupational exposure to whole-body vibration," Journal of Occupational Health, Japan Society for Occupational Health, vol. 58, pp. 118-127, 2016.

[12] B. Erdem1, T. Dog˘an, and Z. Duran, "Assessment of whole-body vibration exposure of mining truck drivers," The Journal of the Southern African Institute of Mining and Metallurgy, vol. 120, pp. 547-539, 2020, doi: 10.17159/2411-9717/1146/2020.

[13] A. Heidarian and X. Quang, "Review on Seat Suspension System Technology Development," Applied Sciences, MDPI, vol. 9, 2019.

[14] L. Zhao, Y. Yu, and C. Zhou, "Comparative research on optimal damping matching of seat system for an off-highway dump truck," International Journal of Engineering, vol. 31, no. 2, pp. 204-211, 2018.

[15] P. Xie, Y. Che, Z. Liu, and G. Wang, "Research on Vibration Reduction Performance of electromagnetic active seat suspension based on sliding mode control," Sensors, MDPI, vol. 22, 2022.

[16] D. Sekulić and V. Dedović, "The Effect of Stiffness and Damping of the Suspension System Elements on the Optimisation of the Vibrational Behaviour of a Bus," International Journal for Traffic and Transport Engineering, pp. 231-244, 2011.

[17] Y. Zhao, M. Alashmori, F. Bi, and X. Wang, "Parameter identification and robust vibration control of a truck driver's seat system using multi-objective optimization and genetic algorithm," Applied Acoustics, vol. 173, pp. 1-13, 2021.

[18] X. Wang, F. Bi, and H. Du, "Reduction of low frequency vibration of truck driver and seating system through system parameter identification, sensitivity analysis and active control," Mechanical Systems and Signal Processing, vol. 105, pp. 1-20, 2018.

[19] M. P. Nagarkar, G. J. V. Patil, and R. N. Z. Patil, "Optimization of nonlinear quarter car suspension–seat–driver model," Journal of Advanced Research, vol. 7, pp. 991-1007, 2016.

[20] M. P. Nagarkar, Y. J. Bhalerao, G. J. V. Patil, and R. N. Z. Patil, "Multi-Objective Optimization of Nonlinear Quarter Car Suspension System – PID and LQR Control," Procedia Manufacturing, vol. 20, pp. 420-427, 2018.

[21] Haiping Du, Weihua Li, Nong Zhang, "Semi-active control of an integrated full-car suspension with seat suspension and driver body model using ER dampers," International Journal of Vehicle Design, vol. 63, pp. 159-184, 2013.

[22] N. Donghong, "An Active Seat Suspension Design for Vibration Control of Heavy-Duty Vehicles," Journal of Low Frequency Noise, Vibration and Active Control, 2016

[23] International Organization for Standardization (ISO). "Mechanical vibration – Road surface profiles – Reporting of measured data." Switzerland. Standard No. ISO 8608. ISO, 2016

[24] Trần Hữu Nhân, Động lực học ứng dụng trong ô tô, mô hình hóa và tính toán mô phỏng, VNUHCM, 2002, pp. 97-170